

How Great is Greater Tuberosity? – A Analysis by CT Multiplanar Reconstruction

Zhiyao Li

Capital Medical University Affiliated Beijing Friendship Hospital

Lifeng Ma

Capital Medical University Affiliated Beijing Friendship Hospital

Wei Yin

Capital Medical University Affiliated Beijing Friendship Hospital

Yingjie Wu

Capital Medical University Affiliated Beijing Friendship Hospital

Zhengrong Qi

Capital Medical University Affiliated Beijing Friendship Hospital

Bo Yang

Capital Medical University Affiliated Beijing Friendship Hospital

Jingxin Zhang

Capital Medical University Affiliated Beijing Friendship Hospital

Qiang Li

Capital Medical University Affiliated Beijing Friendship Hospital

Ai Guo (✉ guoai@ccmu.edu.cn)

Capital Medical University Affiliated Beijing Friendship Hospital

Research article

Keywords: greater tuberosity, computer tomography, multiplanar reconstruction, quantitative radiography

Posted Date: May 28th, 2021

DOI: <https://doi.org/10.21203/rs.3.rs-545901/v1>

License:   This work is licensed under a Creative Commons Attribution 4.0 International License.

[Read Full License](#)

Abstract

Objective: This study was designed to explore the precise size of the greater tuberosity of humerus in Chinese population.

Methods: The radiologic study was performed on 66 CTs of shoulder from the hospital's CT scan database of out-patient department from December 2018 to February 2020. This study designed a method to measure the size of the greater tuberosity (GT). The width, height and thickness of the greater tuberosity were measured on CT image multiplanar reconstructions (MPR), which was independently conducted by two observers.

Results: 66 intact shoulders CT scans were analyzed, including 26 women and 40 men with a mean age of 36.79 ± 9.17 years, with 41 right and 25 left shoulders. There were no significant differences in GT width, GT height, GT thickness and PH thickness between two observers. The ICC for the GT width measurements taken by CT was 0.872. The ICC for the GT height was 0.810. The ICC for the GT thickness was 0.777. The ICC for the PH thickness was 0.971. For male cases, the total PH thickness was 51.06 ± 2.30 (45.70-55.20) mm for female cases, the total PH thickness was 45.79 ± 2.57 (41.40-51.25) mm. Gender have a significant impact on the results, man had a larger GT than woman.

Conclusions: The method was an applicable way the measure the size of greater tuberosity, it showed good reliability. The size of GT in male cases was larger than female. These data provides important information for further research and clinical practice.

Introduction

Greater tuberosity (GT) is an important structure of the proximal humerus. It plays an important role in treatment of fracture, sports injury and degenerative rotator cuff injury. Understanding the size of the great tuberosity was critical in the process of surgery. For example, when performing arthroscopic greater tuberopectomy, there was not a criterion how much bone should be burnished [1]. There was no report about measurement of the precise size about greater tuberosity. There were several study reporting methods of bone structure measurement, including computed tomography (CT), 3D-CT imaging and magnetic resonance imaging (MRI) [2–4]. Most of these studies reported methods by CT measurement and multiplanar reconstruction (MPR) [5]. In addition to the reconstruction of coronal and sagittal planes commonly used in clinic, it can also be used for multi-directional adjustment and MPR. In clinical practice, negative MPR can exclude a diagnosis of tracheobronchial rupture [6]. MPR will be useful for conclusively differentiating this disease from transmesosigmoid hernia [7, 8]. We did not find any studies of the measurement of greater tuberosity by MPR. This study was designed to explore the precise size of the greater tuberosity of humerus in Chinese people by MPR.

In the field of behavioral sciences, the intraclass correlation coefficient (ICC) has been a common parameter or index used to estimate measurement reliabilities induced by human errors and variations among judges or raters. In the neuroimaging field, numerous groups have adapted different forms of ICC

for assessing test-retest reliability in different applications of functional brain imaging [9, 10]. Braun et al. used ICC (3,1) and ICC (2,1) to study the reliability of a functional magnetic resonance imaging (fMRI)-based graph theoretical approach [11]. In this study, ICC was used to quantify the reliability of MPR for measuring GT.

Methods

Subjects

This was a retrospective study, with ethical permission by the ethical committee of Beijing Friendship Hospital (No. 2020-P2-153-01). The data came from the department of radiology. CT Digital Imaging was screened from December 2018 to February 2020. Patients had shoulder CT examination because of shoulder pain or injuries around shoulder. Inclusion criteria were that CT showed normal structure of GT and humeral head, and age of 18-50, both left and right shoulders. Patients selected for this study were not older than 50 years, because patients older than 50 years may develop osteophytes, which may interfere with the measurement results. Exclusion criteria were proximal humeral fracture, arthritis around the greater tuberosity which interfere with the measurement of the morphology, or a humerus shaft was not perpendicular to the scanning plane which had a tilt angle more than 18° on the surview (**Fig 1**).

CT Technique

All shoulder CT scans were performed on a 128/DE CT Scanner (Ingenuity CT, Philips Medical Systems, Cleveland, USA). The scanning parameters were as follows: helical scan type, tube voltage 120 KV, tube current 401 mA, scanning layer thickness and layer spacing 0.5 mm, matrix 512×512, pixels field of view (FOV) 32.9 cm×29.3 cm and exposure 3.4 s. Due to MPR allows for more accurate identification of bone structure and accurate measurements of size, so we choose it rather than 3D-CT for this study. When examine the shoulder radiograph, the humerus should be placed in the correct direction, that is, the axis perpendicular to the scanning plane (deviation $\leq 18^\circ$, bias $< 5\%$, $\cos 18^\circ = 0.95106$, $\cos 19^\circ = 0.94552$), achieving most standard sagittal and coronal plane (**Fig 1**). In a pilot study, on cadaver humerus, we placed a metal marker on the insertion of the teres minor muscle to locate the precise position (**Fig 2**), due to it was a key point of MPR analysis[8,6,12].

Measurement of Parameters

Images from the initial axial CT data were reconstructed at a 0.5 mm slice thickness in MPR (**Fig 3**). On the sagittal planes A, find the one which shows the most prominent tip of the lesser tuberosity. On the chosen sagittal plane, reconstruct the horizontal plane that perpendicular to the shaft through the tip of the lesser tuberosity. On the horizontal plane B, draw a circle that most match the humeral head. And then draw a line (line a) which connect the center of the circle and the middle point of the cortex of greater tuberosity. Then we reconstruct 30 sagittal planes perpendicular to line a containing the greater tuberosity, with 0.5mm interval. Among these sagittal planes, find the one which shows the prominent teres minor insertion (image C). On image C, draw two lines through the medial and lateral margin of the

greater tuberosity respectively which is parallel to the shaft (line b and line c). Then draw a line perpendicular to the shaft through teres minor insertion (line d). Draw a line e through most prominent tip of the greater tuberosity to line d and perpendicular to line d. Then we reconstruct a coronal plane through line e (image D). On image D, line f was in the center of the shaft. Line g was parallel to line f, and it went through the medial margin of the humeral head. Line h was parallel to line f and went through the lateral margin of the greater tuberosity. Line i was parallel to line f and went through the boundary of humeral head and greater tuberosity.

GT width was defined as the distance between the anterior (the posterior wall of the bicipital groove) and posterior margin (insertion of the teres minor muscle), as shown in **Fig. 3C** between line c and line d. GT Height was defined as the distance between tip of the GT and teres minor insertion, as shown in **Fig. 3C** between line e and line d. GT thickness was defined as the distance between lateral cortex and articular margin, as shown in **Fig. 3D** between line h and line i. The thickness of proximal humerus (PH) was defined as the distance between lateral cortex and articular margin, as shown in **Fig. 3D** between line h and line g. All distances were recorded using an electronic caliper in millimeters by 2 trained, independent radiologists.

Statistical analysis

Statistical analysis was performed with SPSS version 17.0 (IBM Corp, Armonk, NY, USA). All results are expressed as means with 95% confidence intervals (CIs) (lower bound to upper bound). The ICC was calculated to determine the amount of concordance [13]. An ICC of 0.01 was considered poor agreement, 0.01 to 0.2 was considered slight agreement, 0.21 to 0.4 was considered fair agreement, 0.41 to 0.6 was considered moderate agreement, 0.61 to 0.8 was considered substantial agreement, and 0.8 to 1.0 was considered almost perfect agreement. The difference between two observers was analyzed with paired-samples T test. The difference between male and female cases was analyzed with Analysis of Variance (ANOVA). $P < 0.05$ was considered significant.

Results

66 intact shoulder CT scans were included and analyzed. Our population included 26 women and 40 men with a mean age of 36.79 ± 9.17 years (from 18 to 50 years old) with 41 right and 25 left shoulders. All of them showed normal structure of GT and humeral head. There was 62.1% showed soft tissue injuries (41/66), 27.8% showed fractures of the scapula or clavicle (19/66), 9.1% showed fractures of the humeral shaft (6/66).

The GT width was 31.36 ± 2.80 (25.10-37.20) by observer 1 and 31.42 ± 2.87 (26.20-36.90) by observer 2. The average width was 31.39 ± 2.74 (25.65-36.85) mm. The average difference was 1.07 ± 0.97 (0-4.50) mm between the two observers ($t=0.358$, $P=0.722$). The ICC for the GT width measurements taken by CT was 0.872.

The GT height was 27.07 ± 2.64 (19.60-33.40) by observer 1 and 27.15 ± 2.77 (20.70-34.10) by observer 2. The average height was 27.11 ± 2.57 (21.05-33.50) mm. The average difference was 1.25 ± 1.11 (0-5.30) mm between the two observers ($t=0.374$, $P=0.710$). The ICC for the GT width measurements taken by CT was 0.810.

The GT thickness was 11.57 ± 1.32 (9.00-14.50) by observer 1 and 11.33 ± 1.16 (8.80-14.40) by observer 2. The average thickness was 11.45 ± 1.18 (9.15-14.30) mm. The average difference was 0.66 ± 0.52 (0-2.40) mm between the two observers ($t=2.428$, $P=0.018$). The ICC for the GT width measurements taken by CT was 0.777.

The PH thickness was 49.03 ± 3.63 (41.10-55.40) by observer 1 and 48.93 ± 3.47 (41.70-55.20) by observer 2. The average thickness was 48.98 ± 3.53 (41.40-55.20) mm. The average difference was 0.67 ± 0.55 (0~2.50) mm between the two observers ($t=0.913$, $P=0.365$). The ICC for the GT width measurements taken by CT was 0.971 (**Table 1**). The thickness ratio (GT/PH) was found to be 0.24 ± 0.02 (0.17~0.30) by observer 1 and 0.23 ± 0.02 (0.17~0.29) by observer 2. For male cases, the total PH thickness was 51.06 ± 2.30 (45.70-55.20) mm. For female cases, the total PH thickness was 45.79 ± 2.57 (41.40-51.25) mm. Gender has a significant impact on the results, men had a larger GT than women (**Table 2**).

Discussion

Treatment options of massive, irreparable rotator cuff tears (MRCT) include conservative treatment, arthroscopic debridement, subacromial biodegradable spacer, partial rotator cuff repair, tendon transfer procedures, interposition allografts, interposition autografts, superior capsular reconstruction, cuff tear arthropathy (CTA) head arthroplasty, reverse total shoulder arthroplasty [14–18]. Tuberoplasty was one of the treatments for irreparable rotator cuff tears to eliminate pain of the shoulder. There were two kinds of tuberoplasty, non-prosthesis tuberoplasty and prosthesis tuberoplasty. Arthroscopic non-prosthesis tuberoplasty was a relatively mini-invasive and effective way among these procedures, which takes little harm to patients [19–22]. But the problem is that there was not a standard procedure for tuberoplasty, and surgeons had performed this surgery by intuition. This study helps surgeons understand more about the arthroscopic tuberoplasty procedure. Meanwhile, prosthesis tuberoplasty was a possible way to treat MRCT. There was no possible to create an absolutely smooth surface with hands by the current surgical procedure. The best smooth surface can be created by artificial prosthesis [23]. The researchers designed a GT prosthesis for tuberoplasty. However, the designing of the GT prosthesis needs precise data of GT. It was crucial to use MPR for the GT prosthesis.

When performing MPR, there were several details for controlling the error of measurement. On Fig. 3B, the observer needs to find the middle point of the GT cortex. It was difficult to find the precise point for the variation of GT morphology. On Fig. 3B, there were several variations of the teres minor insertion. In most cases, there were two prominences. The inferior prominence was suitable for analysis according to our previous pilot study and previous literature. In other cases with only one prominence, it was relatively easy to locate the insertion site.

When confirming the top of the GT on Fig. 3C, there were two variations. Firstly, there was a prominence; the most superior point is the top of GT. Secondly, there was a flat platform. We choose the middle point of the platform as the top of GT.

In this study, there were prominent differences of GT thickness results between two observers. On Fig. 3D, there were variations of the GT-articular boundary. In some cases, there was an obvious corner on the boundary; it was easy to identify the GT and the articular margin. In other cases, there was only an arc, even a flat transition. It's difficult to identify the boundary. This requires the observer to carefully check the thickness of the cortex. The cortex of the articular bone was obviously thinner than that of GT. There was a transition of the cortex. The cortex transition point was considered as the GT-articular boundary. But there may be a transition zone but a transition point, so there was controversy about the precise boundary. The lowest ICC had reflected this controversy. The thickness ratio (GT/PH) was found to be 0.24 ± 0.02 (0.17–0.30) by observer No. 1 and 0.23 ± 0.02 (0.17–0.29) by observer No. 2. The difference mostly came from the difference of GT-articular boundary confirmation.

There were variations of the lateral GT margin on Fig. 3D. The lateral point could be superiorly on the top, or inferiorly on the lateral cortex. It was not so controversial to confirm the medial and lateral margin of the proximal humerus, so we got the highest ICC in PH measurement.

The authors acknowledge several limitations of this study. Defining the dimensions of GT in CT scan is a difficult task due to its irregular shape. The main challenge in this study is to identify the bony landmarks of the teres minor on the CT scan images. There would be some bias though there was a pilot cadaveric study. There may be more accurate method by other researchers by future. In order to reduce measurement errors during the study, all data in the study were completed by two independent observers. We will try our best to improve it in future studies.

Conclusions

The method mentioned in this study has shown good reliability in measuring GT size. The size of GT in male cases was larger than female. These data provides important information for arthroscopic tuberooplasty and design of GT prosthesis.

Abbreviations

greater tuberosity (GT), multiplanar reconstructions (MPR), computed tomography (CT), magnetic resonance imaging (MRI), intraclass correlation coefficient (ICC).

Declarations

Ethical Approval and Consent to participate

The Institutional Review Board of Beijing Friendship Hospital (No. 2020-P2-153-01) approved this study, and all participants signed an approved informed-consent form. All procedures were performed in accordance with the World Medical Association's Declaration of Helsinki.

Consent for publication

All of participants were given written informed consent.

Availability of Data and Materials

All data generated or analysed during this study are included in this published article.

Conflict of interest

The authors declare no conflict of interest.

Acknowledgement

None.

Funding

None.

Authors' contributions

LZY and MLF conceived of the study, and participated in data collection and interpretation of the results and writing of the manuscript. YW, QZR and GA contributed to data collection. YB, LQ and ZJX interpreted the results and writing of the manuscript. All authors read and approved the final manuscript and consented to publish this manuscript.

References

1. Fenlin JM, Jr., Chase JM, Rushton SA, Frieman BG Tubero-plasty: creation of an acromiohumeral articulation-a treatment option for massive, irreparable rotator cuff tears. *J Shoulder Elbow Surg* 2002,11:136-42.
2. Obert L, Peyron C, Boyer E, Menu G, Loisel F, Aubry S CT scan evaluation of glenoid bone and pectoralis major tendon: interest in shoulder prosthesis. *Sicot j* 2016,2:33.
3. Imma, II, Nizlan NM, Ezamin AR, Yusoff S, Shukur MH Coracoid Process Morphology using 3D-CT Imaging in a Malaysian Population. *Malays Orthop J* 2017,11:30-5.
4. Seitlinger G, Scheurecker G, Högl R, Labey L, Innocenti B, Hofmann S Tibial tubercle-posterior cruciate ligament distance: a new measurement to define the position of the tibial tubercle in patients with patellar dislocation. *Am J Sports Med* 2012,40:1119-25.

5. Langerhuizen DWG, Bergsma M, Selles CA, Jaarsma RL, Goslings JC, Schep NWL, Doornberg JN Diagnosis of dorsal screw penetration after volar plating of a distal radial fracture. *Bone Joint J* 2020,102-b:874-80.
6. Chafik D, Galatz LM, Keener JD, Kim HM, Yamaguchi K Teres minor muscle and related anatomy. *J Shoulder Elbow Surg* 2013,22:108-14.
7. Nagano H, Goi T, Taguchi S, Tsubaki T, Uematsu H Diagnosis of incarcerated intramesosigmoid hernia aided by multiplanar reconstruction images of multidetector computed tomography: a case report. *Surg Case Rep* 2018,4:128.
8. Bacle G, Gregoire JM, Patat F, Clavert P, de Pinieux G, Laulan J, Lakhal W, Favard L Anatomy and relations of the infraspinatus and the teres minor muscles: a fresh cadaver dissection study. *Surg Radiol Anat* 2017,39:119-26.
9. Bhambhani Y, Maikala R, Farag M, Rowland G Reliability of near-infrared spectroscopy measures of cerebral oxygenation and blood volume during handgrip exercise in nondisabled and traumatic brain-injured subjects. *J Rehabil Res Dev* 2006,43:845-56.
10. Plichta MM, Herrmann MJ, Baehne CG, Ehlis AC, Richter MM, Pauli P, Fallgatter AJ Event-related functional near-infrared spectroscopy (fNIRS): are the measurements reliable? *Neuroimage* 2006,31:116-24.
11. Braun U, Plichta MM, Esslinger C, Sauer C, Haddad L, Grimm O, Mier D, Mohnke S, Heinz A, Erk S, Walter H, Seiferth N, Kirsch P, Meyer-Lindenberg A Test-retest reliability of resting-state connectivity network characteristics using fMRI and graph theoretical measures. *Neuroimage* 2012,59:1404-12.
12. Vosloo M, Keough N, De Beer MA The clinical anatomy of the insertion of the rotator cuff tendons. *Eur J Orthop Surg Traumatol* 2017,27:359-66.
13. Su P, Jian N, Mao B, Zhang Z, Li J, Fu W Defining the role of TT-TG and TT-PCL in the diagnosis of lateralization of the Tibial tubercle in recurrent patellar dislocation. *BMC Musculoskelet Disord* 2021,22:52.
14. Carver TJ, Kraeutler MJ, Smith JR, Bravman JT, McCarty EC Nonarthroplasty Surgical Treatment Options for Massive, Irreparable Rotator Cuff Tears. *Orthop J Sports Med* 2018,6:2325967118805385.
15. Clark NJ, Elhassan BT The Role of Tendon Transfers for Irreparable Rotator Cuff Tears. *Curr Rev Musculoskelet Med* 2018,11:141-9.
16. Valenti P Joint-preserving treatment options for irreparable rotator cuff tears. *Orthopade* 2018,47:103-12.
17. Gupta AK, Hug K, Boggess B, Gavigan M, Toth AP Massive or 2-tendon rotator cuff tears in active patients with minimal glenohumeral arthritis: clinical and radiographic outcomes of reconstruction using dermal tissue matrix xenograft. *Am J Sports Med* 2013,41:872-9.
18. Mihata T, Lee TQ, Watanabe C, Fukunishi K, Ohue M, Tsujimura T, Kinoshita M Clinical results of arthroscopic superior capsule reconstruction for irreparable rotator cuff tears. *Arthroscopy* 2013,29:459-70.

19. Lee BG, Cho NS, Rhee YG Results of arthroscopic decompression and tuberoasty for irreparable massive rotator cuff tears. *Arthroscopy* 2011,27:1341-50.
20. Park JG, Cho NS, Song JH, Baek JH, Rhee YG Long-term outcome of tuberoasty for irreparable massive rotator cuff tears: is tuberoasty really applicable? *J Shoulder Elbow Surg* 2016,25:224-31.
21. Mirzayan R, Stone MA, Batech M, Acevedo DC, Singh A Failed Dermal Allograft Procedures for Irreparable Rotator Cuff Tears Can Still Improve Pain and Function: The "Biologic Tuberoasty Effect". *Orthop J Sports Med* 2019,7:2325967119863432.
22. Mirzaee F, Aslani MA, Zafarani Z, Aslani H Treatment of Massive Irreparable Rotator Cuff Tear with Arthroscopic Subacromial Bursectomy, Biceps tenotomy, and Tuberoasty. *Arch Bone Jt Surg* 2019,7:263-8.
23. Carvalho CD, Andreoli CV, Pochini AC, Ejnisman B Use of cuff tear arthroplasty head prosthesis for rotator cuff arthropathy treatment in elderly patients with comorbidities. *Einstein (Sao Paulo)* 2016,14:520-7.

Tables

Table 1 Size of greater tuberosity by two observers (mm).

	Width	Height	Thickness	PH thickness
No. 1 (n=66)	31.36±2.80 (25.10~37.20)	27.07±2.64 (19.60~33.40)	11.57±1.32 (9.00~14.50)	49.03±3.63 (41.10~55.40)
No. 2 (n=66)	31.42±2.87 (26.20~36.90)	27.15±2.77 (20.70~34.10)	11.33±1.16 (8.8~14.40)	48.93±3.47 (41.70~55.20)
t	0.358	0.374	2.428	0.913
P	0.722	0.710	0.018	0.365
ICC	0.872	0.810	0.777	0.971

Note: GT greater tuberosity, PH proximal humerus

Table 2 Average size of greater tuberosity of men and women (mm).

	Width	Height	Thickness	PH thickness
Male (n=40)	32.75±2.18 (28.55~36.95)	28.12±2.23 (23.95~33.50)	11.86±1.09 (9.25~14.30)	51.06±2.30 (45.70~55.20)
Female (n=26)	29.29±2.15 (25.65~35.80)	25.55±2.31 (21.05~31.70)	10.83±1.03 (9.15~13.35)	45.79±2.57 (41.40~51.25)
F	=28.998	16.810	10.665	38.072
P	<0.001	<0.001	=0.002	<0.001

Note: GT greater tuberosity, PH proximal humerus

Figures

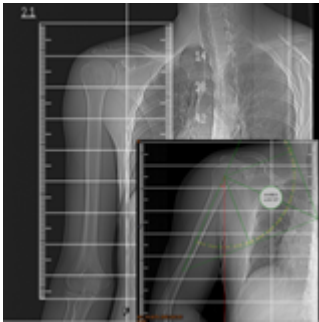


Figure 1

The humerus shaft was perpendicular to the scanning plane on the larger surview, in the smaller surview, the shaft had a tilt angle more than 18°.

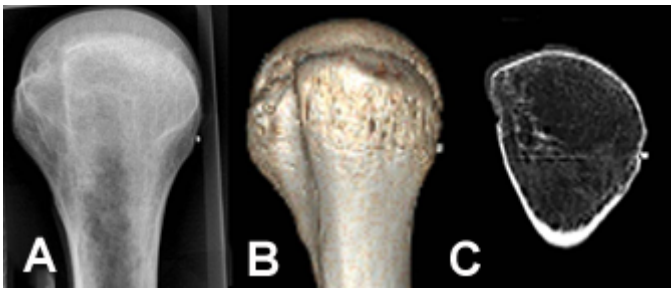


Figure 2

A metal marker on the teres minor insertion. a. plain radiograph of the humeral head, b. 3D image of the humeral head, c. sagittal plane reconstruction of the humeral head.

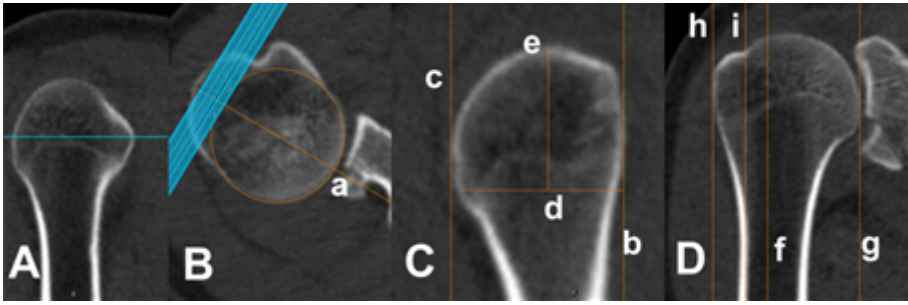


Figure 3

All the details of the reconstruction and measurement.